Resonant Interferometric Lithography beyond the Diffraction Limit

M. Kiffner,[1] J. Evers,[1] and M. S. Zubairy[1,2]

[1]*Max-Planck-Institut für Kernphysik, Saupfercheckweg 1, 69117 Heidelberg, Germany*

[2]*Institute for Quantum Studies and Department of Physics, Texas A&M University, College Station, Texas 77843, USA and Texas A&M University at Qatar, Education City, P. O. Box 23874, Doha, Qatar*

(Received 10 September 2007; published 19 February 2008)

A novel approach for the generation of subwavelength structures in interferometric optical lithography is described. Our scheme relies on the preparation of the system in a position dependent trapping state via phase shifted standing wave patterns. Since this process only comprises resonant atom-field interactions, a multiphoton absorption medium is not required. The contrast of the induced pattern does only depend on the ratios of the applied field strengths such that our method in principle works at very low laser intensities.

DOI: 10.1103/PhysRevLett.100.073602 PACS numbers: 42.50.St, 42.50.Ct, 42.50.Gy, 85.40.Hp

A fundamental limit to the spatial resolution of the interferometric lithography [1] arises due to diffraction. According to the Rayleigh criterion [2], the smallest feature size achievable with classical uncorrelated light is on the order of half the optical wavelength. A scheme that exhibits a larger resolution than the diffraction limit is not only interesting from a fundamental point of view, but also relevant for the semiconductor industry that strives for a miniaturization of their devices. Recently, several schemes [3–7] have been proposed to improve the spatial resolution of interferometric lithography beyond the diffraction limit. The approach of quantum lithography [3] is based on entangled photon-number states that are experimentally difficult to generate and sustain. In order to overcome this difficulty, other approaches have been developed that achieve the desired resolution enhancement via classical coherent light pulses [4,5], but suffer from a reduced visibility of the generated structures. In an improved implementation of quantum lithography with classical light [6,7], subwavelength resolution was accomplished by correlating wave vector and frequency in a narrow band multiphoton detection process. All of the previously cited schemes are based on an N-photon absorption process and achieve a spatial resolution of $\lambda/(2N)$, where λ is the wavelength of the light. The indispensable requirement of a multiphoton transition, however, is accompanied by the need for high light field intensities which makes an experimental realization of these schemes impractical.

Here, we propose a novel method that allows us to achieve the same spatial resolution $\lambda/(2N)$ as previous schemes, but does not require an N-photon absorption process. On the contrary, our scheme relies on the preparation of the system in a position dependent trapping state via phase shifted standing wave patterns and employs resonant atom-field interactions only. In our case, the wavelength corresponds to the spatial period of the incident standing waves, and N specifies the extent of the relevant level scheme (see Fig. 1). We find that the contrast of the induced pattern does only depend on the ratios of the applied laser field strengths, such that in principle, a near-perfect contrast can be achieved with very low laser intensities.

As in previous schemes, we aim at a spatial modulation of the probability to find the atoms in a particular state. For the purpose of lithography, the atoms represent a model for a photoresist that is etched after the exposure has been completed. But in contrast to other schemes, our method to prepare the atoms in a position dependent state relies on the phenomenon of coherent population trapping (CPT) [8,9], and will thus turn out to be fundamentally different from previous approaches. In its simplest case, CPT occurs in a three-level Λ type system as shown in Fig. 1(a). The two stable ground states $|g_1\rangle$ and $|g_2\rangle$ are resonantly coupled to

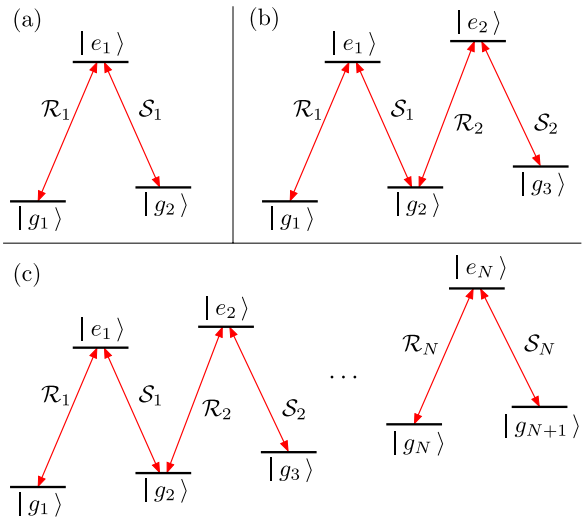

FIG. 1 (color online). Considered level schemes of the photoresist. The ground states $|g_n\rangle$ and $|g_{n+1}\rangle$ are resonantly coupled to the excited state $|e_n\rangle$ via Rabi frequencies $\mathcal{R}_n$ and $\mathcal{S}_n$, respectively. Each excited state $|e_n\rangle$ decays to the ground states $|g_n\rangle$ and $|g_{n+1}\rangle$ by spontaneous emission. (a) Single Λ system. In (b), a sequence of two Λ systems is displayed. (c) General level scheme with N excited and $N+1$ ground states as a sequence of N Λ-type systems.

the excited state $|e_1\rangle$ by laser fields with Rabi frequencies $\mathcal{R}_1$ and $\mathcal{S}_1$, respectively. In this configuration, the system is optically pumped into a coherent superposition of the two ground states which is decoupled from the applied light fields. This so-called dark state is

$$|D_\Lambda\rangle = (\mathcal{S}_1|g_1\rangle - \mathcal{R}_1|g_2\rangle)/\sqrt{|\mathcal{S}_1|^2 + |\mathcal{R}_1|^2}. \quad (1)$$

In our scheme, we suppose that $\mathcal{R}_1$ and $\mathcal{S}_1$ represent standing waves in z direction with wave number $k_0 = 2\pi/\lambda_0$ that are formed by plane waves incident on the substrate, see Fig. 2(a). From Eq. (1), it is clear that the population of each ground state in $|D_\Lambda\rangle$ depends on the ratio of the Rabi frequencies $\mathcal{R}_1$ and $\mathcal{S}_1$. A spatial modulation of the ground state population can thus be obtained if the standing waves corresponding to $\mathcal{R}_1$ and $\mathcal{S}_1$ are phase shifted with respect to each other such that the ratio $\mathcal{R}_1/\mathcal{S}_1$ becomes position dependent. If the two standing waves are phase shifted by $\pi/2$,

$$\mathcal{R}_1 = \Omega_0 \sin(k_0 z + \pi/2), \qquad \mathcal{S}_1 = \Omega_0 \sin(k_0 z), \quad (2)$$

the populations of $|g_1\rangle$ and $|g_2\rangle$ in $|D_\Lambda\rangle$ display the same spatial modulation as the intensity profiles of the standing waves corresponding to $\mathcal{S}_1$ and $\mathcal{R}_1$, respectively,

$$|\langle g_1|D_\Lambda\rangle|^2 = \frac{|\mathcal{S}_1|^2}{|\mathcal{R}_1|^2 + |\mathcal{S}_1|^2} = [1 - \cos(2k_0 z)]/2, \quad (3a)$$

$$|\langle g_2|D_\Lambda\rangle|^2 = \frac{|\mathcal{R}_1|^2}{|\mathcal{R}_1|^2 + |\mathcal{S}_1|^2} = [1 + \cos(2k_0 z)]/2. \quad (3b)$$

The result in Eq. (3) demonstrates that a spatial modulation of the ground state populations can be achieved by means of resonant laser fields. It is important to note that the populations in Eq. (3) do not depend on the maximal Rabi frequency $|\Omega_0|$, but only on the ratio of the Rabi frequencies $\mathcal{R}_1$ and $\mathcal{S}_1$. Thus, the scheme in principle works for very low laser intensities. This illustrates the fundamental difference to previous schemes: Our setup is not bound to nonlinear transition amplitudes between different states such as in the case of multiphoton transitions, which require strong fields. Rather, we exploit the nonlinear dependence of the ground state population probabilities on the Rabi frequencies, which only depends on relative field strengths. As the main result of this Letter, we will show that the above analysis for a single Λ type three-level system can be generalized to level schemes with an $N \times \Lambda$ structure [Fig. 1(c)], where spatial oscillations of a ground state population with wave number $2Nk_0$ and near-complete visibility can be achieved.

We also note that for unequal amplitudes of the Rabi frequencies of the standing wave fields, a single very narrow spatial structure at a controllable position within a range of $\lambda/2$ can be generated, which could be used to write desired structures point by point.

We start our analysis by illustrating the general idea on the basis of the $2 \times \Lambda$ or M system shown in Fig. 1(b). The generalization of the dark state Eq. (1) for this system under the influence of the driving fields $\mathcal{S}_n$ and $\mathcal{R}_n$ ($n \in \{1, 2\}$) is given by [10]

$$|D_{2\times\Lambda}\rangle = (\mathcal{S}_1\mathcal{S}_2|g_1\rangle - \mathcal{R}_1\mathcal{S}_2|g_2\rangle + \mathcal{R}_1\mathcal{R}_2|g_3\rangle)/\sqrt{C_2}, \quad (4)$$

where C_2 is the normalization constant [see Eq. (7)]. It follows that the probability to find the system in state $|g_1\rangle$ is proportional to $|\mathcal{S}_1\mathcal{S}_2|^2$, which involves the product of the fields $\mathcal{S}_1$ and $\mathcal{S}_2$. If both $\mathcal{S}_1$ and $\mathcal{S}_2$ display a sinusoidal oscillation with respect to position, i.e., $\mathcal{S}_1 \sim \sin(k_0 z)$ and $\mathcal{S}_2 \sim \sin(k_0 z + \phi)$, we obtain $|\mathcal{S}_1\mathcal{S}_2|^2 \sim [\cos(\phi) - \cos(2k_0 z + \phi)]^2$. Choosing the relative phase shift of the two standing waves as $\phi = \pi/2$, we find $|\mathcal{S}_1\mathcal{S}_2|^2 \sim [1 - \cos(4k_0 z)]/2$. Thus, population oscillations with wave number $4k_0$ are obtained, while the contribution with

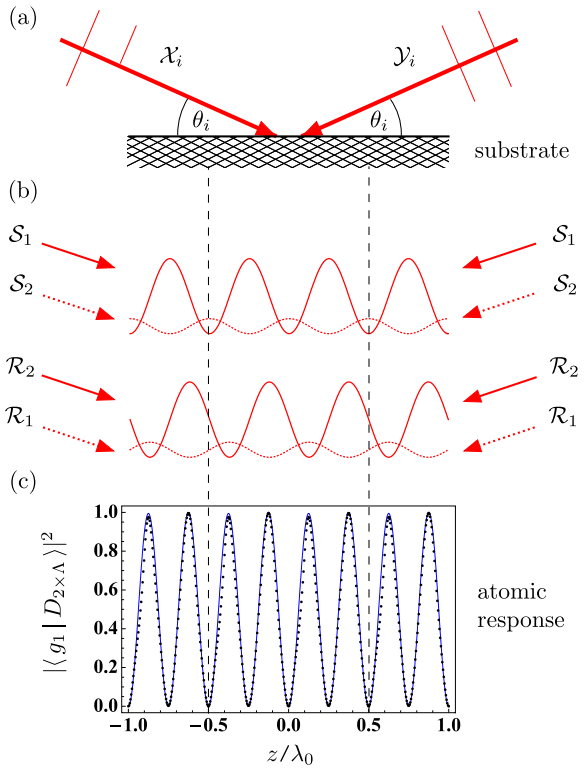

FIG. 2 (color online). (a) Each standing wave pattern $\mathcal{R}_n$, $\mathcal{S}_n$ is formed by two plane waves $\mathcal{X}_i$, $\mathcal{Y}_i$ with wavelength λ_i. The period of each intensity pattern is given by $\lambda_0/2$, where $\lambda_0 = \lambda_i/\cos\theta_i$, and θ_i is chosen such that the effective wavelength in the substrate plane is equal to λ_0 for all $\mathcal{R}_n$ and $\mathcal{S}_n$. Subfigures (b) and (c) correspond to the M system shown in Fig. 1(b). Part (b) illustrates the intensity profiles of the standing waves $\mathcal{R}_n$ and $\mathcal{S}_n$ ($n = 1, 2$) according to Eq. (9). Note that $|\mathcal{R}_n|^2$ and $|\mathcal{S}_n|^2$ are not drawn to scale. The solid line in (c) shows the population of state $|g_1\rangle$ corresponding to Eqs. (10) and (12) with $\eta = 1/20$. It varies with wave number $4k_0$. The dotted line is the corresponding result with nonzero ground state decoherence rates γ_{coh}. We set $\gamma_{\text{coh}} = \gamma$, where γ is the full decay rate on the $|e_n\rangle \leftrightarrow |g_{n\pm1}\rangle$ transition.

wave number $2k_0$ has been canceled, see Fig. 2. Note that for the moment we have neglected the normalization constant C_2 in Eq. (4) that generally depends on position.

We now turn to the general level scheme in Fig. 1(c). In the interaction picture and in rotating-wave approximation, the interaction Hamiltonian of the $N \times \Lambda$ system takes the form

$$H_{N\times\Lambda} = \hbar \sum_{n=1}^{N} (\mathcal{R}_n |e_n\rangle\langle g_n| + \mathcal{S}_n |e_n\rangle\langle g_{n+1}| + \text{H.c.}), \quad (5)$$

where H.c. denotes the Hermitian conjugate. We assume that the resonance frequencies of the various transitions are sufficiently distinct such that the Rabi frequencies $\mathcal{R}_n$ and $\mathcal{S}_n$ can be chosen individually. The dynamics of the atomic density operator can be described by a master equation $\partial_t \varrho = -i[H_{\text{int}}, \varrho]/\hbar + \mathcal{L}_\gamma \varrho$, where $\mathcal{L}_\gamma$ accounts for spontaneous emission of the N excited states to the ground states. We assume that each excited state $|e_n\rangle$ decays to both ground states $|g_n\rangle$ and $|g_{n+1}\rangle$. In order to avoid singular cases where the steady state of the system depends on the initial condition, we require that either all Rabi frequencies $\mathcal{R}_n$ or all $\mathcal{S}_n$ ($1 \le n \le N$) are different from zero at any point in space. Then, the steady state of the system evaluates to the following superposition of ground states [11],

$$|D_{N\times\Lambda}\rangle = \frac{1}{\sqrt{C_N}} \sum_{n=1}^{N+1} (-1)^{n+1} \prod_{k=1}^{n-1} \mathcal{R}_k \prod_{j=n}^{N} \mathcal{S}_j |g_n\rangle, \quad (6)$$

where

$$C_N = \sum_{n=1}^{N+1} \prod_{k=1}^{n-1} |\mathcal{R}_k|^2 \prod_{j=n}^{N} |\mathcal{S}_j|^2 \quad (7)$$

is the normalization constant and we set $\prod_{k=1}^{0} = \prod_{j=N+1}^{N} = 1$. Thus, as in the case of the single Λ system, the atoms are optically pumped into a dark state $|D_{N\times\Lambda}\rangle$. From now on, we suppose that the atoms have reached this steady state.

The key ingredient of our scheme is that a product of N sinusoidal waves with wave number k_0 can display spatial oscillations with wave number Nk_0 only. All other harmonics with wave number nk_0 with $n \le N$ can be canceled with a suitable choice of the relative phase shifts of the standing waves. Formally, this property is described by the trigonometric identities

$$\prod_{n=1}^{N} \sin[k_0 z + (n-1)\pi/N] = \frac{\sin(Nk_0 z)}{2^{N-1}}, \quad (8a)$$

$$\prod_{n=1}^{N} \sin[k_0 z + (2n-1)\pi/(2N)] = \frac{\cos(Nk_0 z)}{2^{N-1}}. \quad (8b)$$

The application of these identities to our system is straightforward. For this, we notice that the coefficient of $|g_1\rangle$ in the expansion of the dark state in Eq. (6) is proportional to the product of all Rabi frequencies $\mathcal{S}_n$, i.e., $\langle g_1|D_{N\times\Lambda}\rangle \sim \prod_{n=1}^{N} \mathcal{S}_n$. Similarly, the matrix element $\langle g_{N+1}|D_{N\times\Lambda}\rangle \sim \prod_{n=1}^{N} \mathcal{R}_n$ involves the product of all Rabi frequencies $\mathcal{R}_n$. If we choose the position dependence of $\mathcal{R}_n$ and $\mathcal{S}_n$ according to

$$\mathcal{S}_n(z) = S_n \sin[k_0 z + (n-1)\pi/N], \quad (9a)$$

$$\mathcal{R}_n(z) = R_n \sin[k_0 z + (2n-1)\pi/(2N)], \quad (9b)$$

it follows from Eqs. (6) and (8) that we have

$$|\langle g_1|D_{N\times\Lambda}\rangle|^2 = A_1[1 - \cos(2Nk_0 z)]/2, \quad (10a)$$

$$|\langle g_{N+1}|D_{N\times\Lambda}\rangle|^2 = A_{N+1}[1 + \cos(2Nk_0 z)]/2. \quad (10b)$$

Thus, with our choice Eq. (9) on first sight, only spatial oscillations with wave number Nk_0 are retained, as desired. But as mentioned before, in general the amplitudes $A_1 = \prod_{n=1}^{N} |S_n|^2/(C_N 4^{N-1})$ and $A_{N+1} = \prod_{n=1}^{N} |R_n|^2/(C_N 4^{N-1})$ also depend on position via the normalization constant C_N in Eq. (7). Furthermore, for a full population oscillation amplitude required for a high lithography contrast, the amplitudes A_1 and A_{N+1} should ideally be equal to unity. To a very good approximation, this goal can be achieved if the parameters R_n and S_n in Eq. (9) are chosen according to

$$|R_1| = |S_N| = \eta\Omega_0, \qquad 0 < \eta \ll 1, \quad (11a)$$

$$|R_N| = |S_1| = |R_n| = |S_n| = \Omega_0, \qquad 1 < n < N, \quad (11b)$$

where Ω_0 is an arbitrary positive Rabi frequency. Thus, the laser fields driving the outermost ground states should be much weaker than all other fields. The amplitudes A_1 and A_{N+1} are then given by

$$A_1 = A_{N+1} = 1/[1 + \eta^2 f_N(z)], \quad (12)$$

where the function f_N is independent of η and will not be given here. It follows from Eq. (12) that $A_1 \approx A_{N+1} \approx 1$ if the parameter η is much smaller than unity.

Equations (10) and (12) represent the main result of this Letter and demonstrate that a sinusoidal oscillation in space of the population of states $|g_1\rangle$ and $|g_{N+1}\rangle$ with wave number $2Nk_0$ can be achieved, provided that the Rabi frequencies $\mathcal{R}_n$ and $\mathcal{S}_n$ are chosen according to Eqs. (9) and (11). Also in the general case, we find from Eq. (11) that our approach does not require strong laser fields, since the maximal Rabi frequency Ω_0 can be chosen arbitrarily and cancels out in the final result. Terms that describe deviations from perfect sinusoidal oscillations between zero and unity are at most on the order of η^2, which can be neglected for practical applications provided that the relative laser field intensities are chosen appropriately. Note that the population of the remaining ground states $|g_n\rangle$ ($1 < n \le N$) are also suppressed by a factor of η^2. An illustration of our results for $N = 2$ is presented in Fig. 2(c), where the solid line shows the spatial oscillation of the population of $|g_1\rangle$ according to Eqs. (10) and (12).

The CPT mechanism itself relies on the preservation of the ground state coherence in order to evolve into the stationary dark state. But even a large ground state decoherence rate γ_{coh} does not affect the applicability of our scheme. In Fig. 2(c), the dotted curve shows the result for the same parameters as the solid line, but with γ_{coh} set equal to the population decay rate γ on the dipole-allowed transitions from the excited to the ground states. It can be seen that the results virtually coincide. Only with γ_{coh} exceeding γ, we find a noticeable decrease in the visibility of parts of the peak structure. This surprising result can be understood by noting that key features like the minima in Fig. 2(c) arise from optical pumping alone without the need for CPT. Once the steady state has been reached, the light fields can be switched off, as the populations are not affected by the loss of coherence.

So far, we required all wave numbers of the standing waves $\mathcal{R}_n$ and $\mathcal{S}_n$ to be identical to k_0, see Eq. (9). But also, the frequencies of the fields $\mathcal{R}_n$ and $\mathcal{S}_n$ are supposed to be different for individual addressing. Both conditions can be met by choosing the incident angles θ_i appropriately, see Fig. 2(a). This, however, may be challenging in reality, in particular, for $N \times \Lambda$ systems with larger N. Thus, we estimate the influence of a wave vector mismatch and demonstrate that equal incident angles θ for all fields may be sufficient. Writing the wave numbers as $k = k_0 + \Delta k$, the result in Eq. (10) is obtained as the zeroth order term in an expansion in $\epsilon = |\sin(\Delta k z)|$, which is a small parameter provided that $|\Delta k z| \ll 1$, or equivalently $|z/\lambda_0| \ll k_0/(2\pi\Delta k)$. For optical transitions, it is well justified to assume that the frequency difference $\Delta\nu$ between transitions is much smaller than the mean transition frequency $\nu_0 = ck_0/(2\pi)$, even if all transitions are addressed individually. It follows that the inequality $|z/\lambda_0| \ll k_0/(2\pi\Delta k) = \nu_0/(2\pi\Delta\nu)$ and hence the applicability of Eq. (10) even with wave vector mismatch holds in a region around $z = 0$ which typically extends over several hundreds or even thousands of wavelengths. In addition, this working region can be shifted spatially by adding a global phase shift to the standing waves in Eq. (9). Perturbations Δk to k_0 also model instabilities of external parameters such as the laser frequencies.

The realization of our scheme for higher harmonics of the incident writing fields requires an extended energy level scheme. In atomic gases, suitable level structures can be found, e.g., in ^{85}Rb and ^{87}Rb [12]. As in atomic resonance lithography (ARL) [13], the position-dependent population pattern imprinted by the light fields could be used, e.g., to selectively expose a resist on a surface. In contrast to ARL, in our scheme the resolution in principle can be increased via the extend of the level scheme N. A resolution limitation however is given by the center of mass motion of atoms in the gas induced by the atom-light interactions until the steady state is reached. A second potential realization involves the direct exposition of a photoresist on a surface, such that the center of mass motion is irrelevant. Suitable coherence times have already been demonstrated between spin states in doped solids, which may serve as a model system for the resist. Here, a tradeoff between lower temperatures in order to increase the ground state coherence times [14,15] and higher temperatures in order to broaden the linewidth of the individual dopants to bring a large fraction of them in resonance [16] must be found. A considerably larger state space becomes accessible if different vibrational transitions could be utilized [6]. Either way, the applicability of our scheme already at low field intensities considerably facilitates the realization, in particular, in extended systems. A desired 2-dimensional final pattern is achieved via multiple exposure with different harmonics based on a Fourier decomposition [7]. In a medium that supports the generation of oscillations with maximal wave number $2Nk_0$, all smaller wave numbers $2nk_0$ with $0 < n \leq N$ can be generated by appropriately modifying the incident angle θ [4]. The required harmonics can also be generated without changing θ using different $n \times \Lambda$ ($n \leq N$) subsystems of the same full level structure.

M. S. Z. would like to thank the Alexander von Humboldt Foundation for supporting this research.

[1] S. R. J. Brueck, S. H. Zaidi, X. Chen, and Z. Zhang, Microelectron. Eng. **42**, 145 (1998).
[2] Lord Rayleigh, Philos. Mag. **8**, 261 (1879).
[3] A. N. Boto *et al.*, Phys. Rev. Lett. **85**, 2733 (2000); P. Kok *et al.*, Phys. Rev. A **63**, 063407 (2001); G. S. Agarwal, R. W. Boyd, E. M. Nagasako, and S. J. Bentley, Phys. Rev. Lett. **86**, 1389 (2001); M. D'Angelo, M. V. Chekhova, and Y. Shih, *ibid.* **87**, 013602 (2001).
[4] S. J. Bentley and R. W. Boyd, Opt. Express **12**, 5735 (2004).
[5] A. Pe'er *et al.*, Opt. Express **12**, 6600 (2004).
[6] P. R. Hemmer, A. Muthukrishnan, M. O. Scully, and M. S. Zubairy, Phys. Rev. Lett. **96**, 163603 (2006).
[7] Q. Sun, P. R. Hemmer, and M. S. Zubairy, Phys. Rev. A **75**, 065803 (2007).
[8] M. O. Scully and M. S. Zubairy, *Quantum Optics* (Cambridge University Press, Cambridge, 1997).
[9] E. Arimondo, in *Progress in Optics*, edited by E. Wolf (Elsevier, Amsterdam, 1996), Vol. 35, p. 259.
[10] M. S. Zubairy, A. B. Matsko, and M. O. Scully, Phys. Rev. A **65**, 043804 (2002).
[11] A. B. Matsko, I. Novikova, M. S. Zubairy, and G. R. Welch, Phys. Rev. A **67**, 043805 (2003).
[12] V. Balić *et al.*, Phys. Rev. Lett. **94**, 183601 (2005).
[13] J. H. Thywissen and M. Prentiss, New J. Phys. **7**, 47 (2005).
[14] A. V. Turukhin *et al.*, Phys. Rev. Lett. **88**, 023602 (2001).
[15] H. Goto and K. Ichimura, Phys. Rev. A **74**, 053410 (2006).
[16] R. Kolesov, Phys. Rev. A **72**, 051801(R) (2005).